Bulletin of Earth Sciences of Thailand

ROCK PHYSICS AND SEISMIC INVERSION ANALYSIS FOR RESERVOIR IDENTIFICATION IN SW PALAWAN PHILIPPINES

Sheila Marie S. Borbajo*

Petroleum Geoscience Program, Department of Geology, Faculty of Science,
Chulalongkorn University, Bangkok 10330, Thailand
*Corresponding author email: cuteyla@yahoo.com

Abstract

Rock physics analysis and seismic inversion in Service Contract 63, Southwest Palawan Basin, Philippines, has been found to be an effective way to delineate the clastic and carbonate reservoirs within the block. Two types of inversion were conducted, namely, a simultaneous inversion using partial seismic angle stack data for the Pagasa Formation and an acoustic impedance inversion using full stack seismic data for the Nido Limestone. It is difficult to distinguish the sands and shales in the Pagasa Formation but the gas sands could be differentiated from brine sands and shales in the acoustic impedance (AI)-extended elastic impedance (EEI) domain, where two types of gas sands were delineated. The first type corresponds to low AI and high EEI, whereas the second type relates to moderate AI and low EEI and correlates to the interval that flowed 50 MMscfgpd of gas in the Abo Abo-A1X well. The higher AI in the second type of gas sand could be brought about by the presence of limestone fragments in the sands as defined from petrographic analysis. The limestones on the other hand have high AI and correlate to the bright reflectors on seismic data. For the Nido Limestone, low AI values can be correlated to high porosity while higher AI values are associated with lower porosity This predictable relationship between acoustic impedance and carbonate porosities is similar to the reported character of the Nido Limestone in the Northwest Palawan Basin. Seismic inversion is a viable tool that can be used to identify the presence of both clastic and carbonate reservoirs and reduce the exploration risk in the Southwest Palawan Basin.

Keywords: Southwest Palawan Basin, Simultaneous seismic inversion, EEI, Nido Limestone, Pagasa Formation

1. Introduction

The Southwest Palawan Basin is relatively under explored and does not have any commercial hydrocarbon discoveries compared to the adjacent Northwest Palawan Basin, where the producing Nido, Galoc and Malampaya Fields are located. Although the plays tested in both basins are generally similar, the reefal carbonate play on the Nido Limestone proven by the Malampaya and Nido discoveries, and the clastic play on the Pagasa Formation proven by the Galoc discovery, there is less exploration success on the southwest part of the basin. Reservoir presence, quality, and distribution are some of the main risks in the basin. This is further complicated by its more tectonically complex history. Although it could also be argued that the more intense compressional regime could also be beneficial as it provides more opportunities for the generation of structural traps.

The latest well drilled in the basin, the Baragatan-1A well, drilled in 2014 by the Philippine National Oil Company Exploration Corporation (PNOC EC), targeted clastic reservoirs pre-drill but instead encountered carbonates within the Pagasa Formation. It was drilled on bright amplitudes, expecting gas-saturated sands. This well exemplifies the reservoir risk associated with exploration in the basin.

In this study, rock physics analysis and seismic inversion has been proven as an effective technique that provided a robust framework for differentiating sands, shales and carbonates within the Pagasa Formation and distinguishing regions with higher porosities within the Nido Limestone.

1.1 Study Area

The project area (AOI in Figure 1) was focused on 3D seismic data (called Kawayan 3D) acquired in the southernmost portion of Service Contract (SC 63). The acreage is located

offshore, west of the Palawan Island and is about 130 kilometers southwest of the producing oil and gas fields that includes the Camago-Malampaya gas field of Shell and the Nido oil field.

The Abo Abo-A1X well, a gas discovery that flowed 50 million cubic feet of gas per day (MMcfgpd) during a Drill Stem Test (DST) is within the study area. Also included within the project Area of Interest (AOI) are the Albion Head-1, Baragatan-1A, and the Santiago-A1X wells. Water depths within the AOI range from 40 to 1,700 meters.

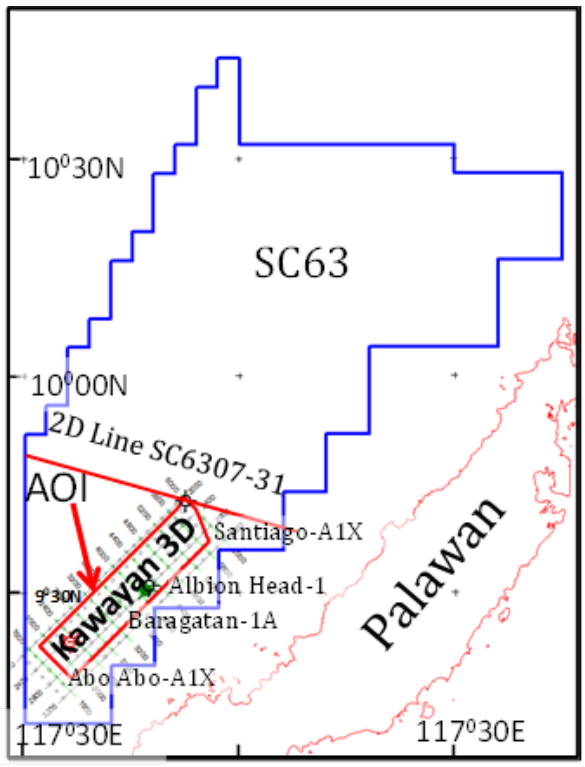

Figure 1. Location map of the study area.

A representative seismic section within the study area is shown in Figure 2. This section also shows the vertical extent of the study which is from Top of the Pagasa Formation to the base of the Nido Limestone.

All the data used in this study were provided by PNOC EC and the software used for the rock physics modelling and seismic inversion was Ikon Science Ltd's RokDoc.

1.2 Objectives

- To establish the rock physics parameters which can differentiate lithology and fluid within the Pagasa and the Nido Formations using well data.
- Conduct simultaneous inversion in Pagasa for lithology and hydrocarbon delineation
- Conduct a P-Impedance seismic inversion in Nido Limestone to determine high porosity zone
- Analyze inversion results and determine potential areas for future exploration

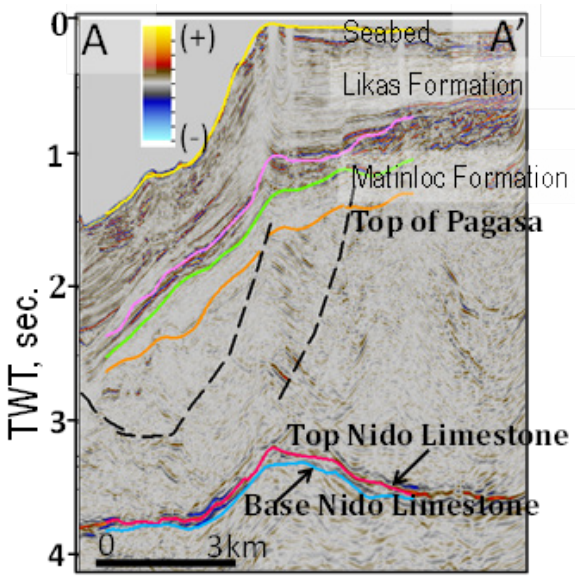

Figure 2. Representative dip line seismic section across the Kawayan 3D showing the interpreted horizons and faults.

1.3 Regional Geology and Tectonics

The Palawan Island, situated on the southeastern edge of the South China Sea, and shelf are comprised of two different blocks, separated by the Ulugan Fault Zone (Steuer et al, 2013). Offshore, the Northwest Palawan Basin lies north of the Ulugan Fault Zone and the Southwest Palawan Basin is situated south of the fault zone. The Southwest Palawan Basin is regarded as an accreted terrane that was thrusted over the thinned leading edge of the rifted Eurasian margin (Forbes et al, 2011).

The generalized stratigraphic column of the basin is shown in Figure 3. The Pagasa Formation in SC63 consists predominantly of claystone, with thin interbeds of siltstone and sandstone.

In the Baragatan-1A well, limestone

interbeds instead of sands were encountered within the Pagasa Formation. According to the Baragatan-1A End of Well Report, limestones were identified as predominantly mudstone to wackestone, with minor grainstone and packestone.

The Nido Limestone on the other hand was described in the core acquired in the Santiago-A1X well as packed coralgal biomicrite to biocalcarenite with abundant coralgal fragments. Porosity is generally poor to fair but where leaching is present, the porosity is good.

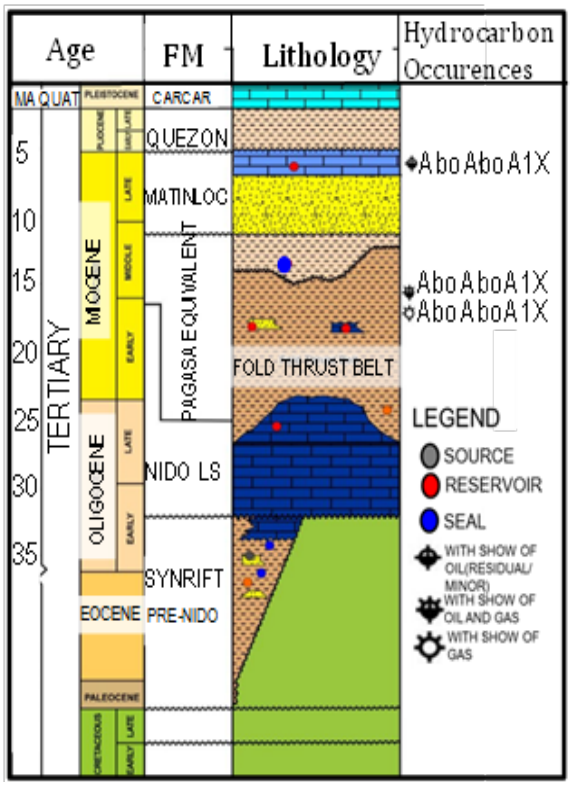

Figure 3. Generalized stratigraphic column of Southwest Palawan (after Forbes et al, 2011)

2. Database

2.1 Seismic Data

The Kawayan 3D seismic data cover an area of approximately 754 square kilometers. Bin spacing is at 18.25m by 6.25m with 2ms sampling rate. The dataset used in this study is the 2012 Beam PSDM data. The full stack and three partial angle stacks (5-15 deg, 15-30, deg, and 30-45 deg) were utilized in the inversion. The seismic data were processed as zero phase and an increase in acoustic impedance is represented as a peak. The frequency bandwidth of the seismic data from the amplitude spectral analysis (6 dB down) is from 6 to 45 Hz, (near), 5 to 40 Hz (mid), 5 to 30 Hz (far) and full 5 to 50 Hz.

2.2 Well Data

Logs, checkshots and formation tops data were supplied for the 4 wells used namely: Abo Abo-A1X, Albion Head-1, Baragatan-1A, and Santiago-A1X.

2.3 Velocity Data

The seismic velocity data came from the final migration velocity of the beam PSDM processing. Inline and crossline spacing is 200 m whereas the vertical sampling is 24ms. The velocity supplied is in Vrms and in the time domain.

3. Methodology

3.1 Rock Physics Analysis

Rock physics analysis of the well data was performed prior to the inversion in order to determine the best rock properties for discriminating lithology and fluid.

Elastic impedance (EI) and extended elastic impedance (EEI) were calculated from the raw log data to check the application of these two properties for lithology and fluid identification.

EEI is an expansion of the EI concept first formulated by Connolly (1999), which is a generalization of acoustic impedance (AI) for non-normal incidence angle, enabling the benefits of inversion to be exploited for AVO data (Whitcombe, 2002). EI is a function of P-velocity (α), S-velocity (β), density (ρ), and the incidence angle (θ);

EI (θ) = $\alpha^a \beta^b \rho^c$, where a = (1 + sin2 θ), b= - 8K sin2 θ, and c = (1 – 4K sin2 θ); K is a constant, usually set to the average value of $(\beta/\alpha)^2$ over the log interval of interest (Whitcombe, 2002).

EEI is a modification by Whitcombe (2002) of EI beyond the range of physically meaningful incidence angle (θ), which is from 0 to about 30 degrees (Shuey, 1985). This was done by substituting tan χ for sin2 θ in the 2

term reflectivity equation (A + B sin2 θ), which allowed χ to range from -90 to 90 degrees and gives an extension of EI for any combination of intercept (A) and gradient (B). The EEI equivalent to χ = 0 deg is AI, and at χ = 90 deg is referred to as gradient impedance (GI).

Cross plots of P-velocity (Vp), S-velocity (Vs), P-Impedance (AI), S-impedance (SI), Density (Rho), Porosity (Por), Elastic Impedance (EI), Extended Elastic Impedance (EEI), with respect to each other and color coded by Volume of shale (Vshale), Gamma ray (GR) and water saturation (Sw) were analyzed to define the physical parameters that will discriminate lithology and fluids.

A Vshale cutoff of < 0.40 was used to define the sands while shales were defined as having Vshale > 0.40.

In order to determine the optimum chi (χ) angles for EEI that best correlates with water saturation and Vshale, a range of normalized EEI logs were calculated at chi angles ranging from -90 to 90 degrees, and the results were plotted in a graph that shows chi angle (χ) versus correlation.

3.3 Seismic Inversion

The simultaneous seismic inversion algorithm using Smith and Gidlow (1987) & Fatti (1994) model was used as this allows the generation of EEI volumes as a product of the inversion aside from the normal acoustic and shear impedance volumes.

The quality control of the inversion was done along the wells before inverting along a line of a section and later on to the full 3D. The misfit is computed by comparing the synthetic model with the original seismic partial angle stacks.

Post stack seismic inversion was used to map the high impedance Nido Limestone. This inversion, however, was complicated by the fact that the only well within the 3D coverage that penetrated the Nido limestone, Santiago-A1X, is located at the edge of the 3D data and in a data wipeout zone. This, therefore, precludes the execution of a proper seismic to well tie and the estimation of the wavelet at the Santiago-A1X well location for the 3D seismic data.

In order to estimate the wavelet, the well was tied to the 2D seismic line passing through the Santiago-A1X well, 2D line SC6307-31 (Figure 1). However, since the 3D data were acquired and processed independently of the 2D data, the amplitude spectrum of the 3D seismic data and the 2D line is different. In order to account for the difference, the wavelet estimated from the 2D data was therefore scaled to match it to the 3D seismic data.

In order to convert the acoustic impedance to porosity, a linear transform based on the AI-Porosity cross plot of the Santiago-A1X well was used.

4. Results

4.1 Rock Physics Analysis

4.1.1 Pagasa Formation

The AI vs SI (Figure 4) and the AI vs Vp/Vs plots (Figure 5) show that the sandstones and shales in the Pagasa Formation are difficult to differentiate by the acoustic and shear impedance domains. There is a significant overlap for sands and shale. The hydrocarbon filled sands have lower AI and SI but these still overlap with some brine sand and shale. The limestones have very high AI.

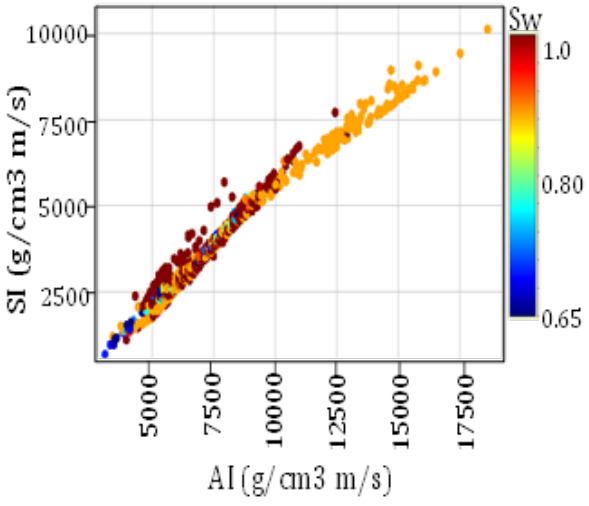

Figure 4. AI vs SI crossplot in the Pagasa Formation.

The elastic impedance (EI) and extended elastic impedance (EEI) properties of the wells were investigated to see if the differentiation

between different fluids could be achieved. The chi (χ) angle of 25 degrees showed the maximum correlation between the EEI and saturation (Figure 6). For the Vshale volume, the highest correlation with EEI was at the chi (χ) angle of 65 degrees. However, the AI vs EEI log (at chi = 65 deg) still does not discriminate the sand from shale. This implies that it is indeed very difficult to differentiate sand from shale in the Pagasa Formation because of their similar acoustic and elastic properties.

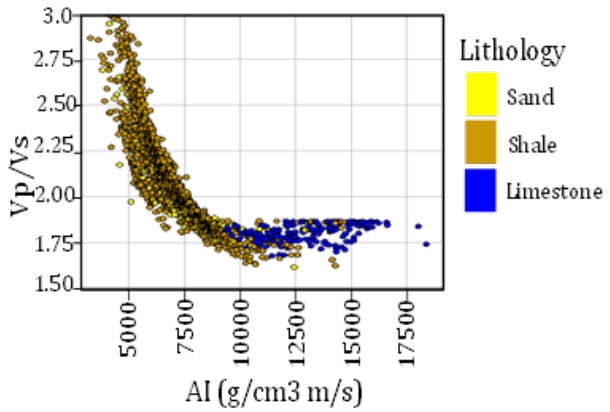

Figure 5. AI vs Vp/Vs crossplot in the Pagasa Formation.

The AI vs EEI (at chi angle 25 deg) plot of the Abo Abo-A1X well (Figure 7) shows that the cross plot of these properties provides more separation between the gas sands, and the brine sands and shales. The Abo Abo-1X well was selected because this is the only well in the dataset that encountered gas, and one of the five drill stem tests (DST) conducted flowed gas at a rate of 50 million standard cubic feet per day (MMscfgpd).

Two types of gas sands were identified in the AI-EEI cross plot, each with distinct acoustic and elastic properties. The first type corresponds to low AI (lower than 5000 g/cm3 m/s) and high EEI (7000 to 7500) and is linked to the sands which were tested in DST5 (Figure 8).

These sands did not flow gas but the gas saturation curves showed gas saturations up to a maximum of about 40 percent. The low AI in these sands matches well to the typical effect of gas on sands which is the lowering of AI due to the very low density and velocity of the gas.

According to the Abo Abo-A1X Biostratigraphic and Petrographic Report (2014), the sample taken at 1823m (5980 feet) is composed of 48% very fine grained arkosic sandstone and 52 % argillaceous siltstone.

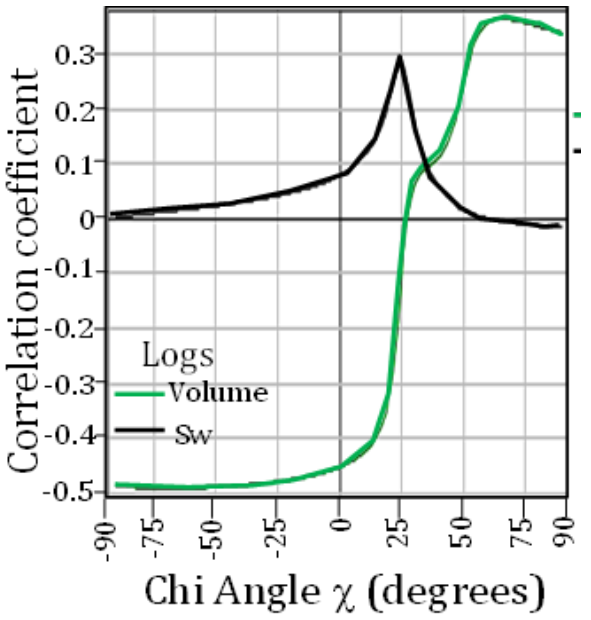

Figure 6. The correlation coefficients between EEI and Sw, and EEI and Vshale curve for a range of values of chi angles.

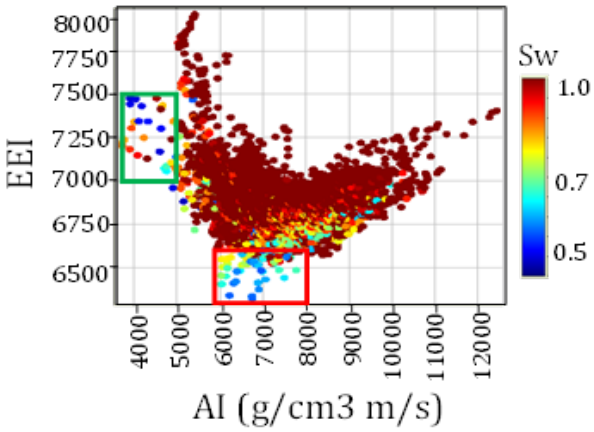

Figure 7. AI-EEI crossplot highlighting the two types of gas sands (rectangles).

The second type of gas sand corresponds to low EEI (lower than 6400) and moderate AI (6000 to 8000 g/cm3 m/s) and correlates to the interval which flowed gas at a rate of 50MMscfpd during a DST (Figure 9c). The AI here is similar in range to the AI of the brine sands and shales and is higher than the first type of gas sands.

The petrographic analysis (Abo Abo-A1X Biostratigraphic and Petrographic Report, 2014) of the sample taken below the tested interval, at 2624m (8610 feet), shows the presence of limestone fragments within the sand. The sample was described as having 42% chert, 40% sandy claystone, 10% calcareous sandstone, and 8% limestone. The AI of this sand has a value of 7800 g/cm3 m/s. The presence of limestone in the second type of gas sands could potentially have caused the increase in its AI value.

Based on the rock physics analysis, a simultaneous inversion of partial seismic angle stacks generating AI and EEI is necessary to distinguish the gas saturated zones from brine sands and shales.

4.1.2 Nido Limestone

The acoustic impedance and porosity in the Nido Limestone has a predictable relationship as shown by the AI vs porosity cross plot in Figure 9. The higher porosity can be correlated to low AI whereas the lower porosity corresponds to higher AI. This AI-porosity relationship is similar to the character of the Nido Limestone in the adjacent Northwest Palawan basin based on published works in the Malampaya gas field (Fournier and Borgomano, 2007) and in Service Contract 54, in the Coron-1 and Pagasa-1 wells (Borbajo, 2010).

A P-impedance seismic inversion using only full stack seismic data is therefore sufficient to determine the high porosity zones within the Nido Limestone.

4.1 Seismic Inversion

4.1.1 Pagasa Formation

Figure 10 shows the seismic to well tie for the Abo Abo-A1X well used in the inversion. A good well tie was achieved for the Abo Abo-A1X and Albion Head-1 wells, with of 66% and 59% correlation coefficient, respectively. A slightly lower correlation coefficient of 41% was achieved for the Baragatan-1A well tie.

In order to check whether the gas sands encountered in the Abo Abo-A1X well were captured in the inversion results, the AI, SI, and

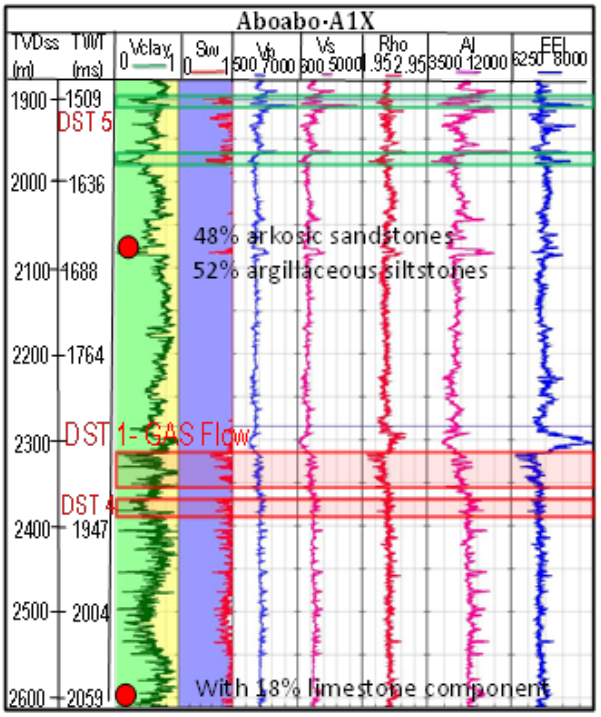

Figure 8. Abo Abo-A1X well log. Depth where samples were taken for petrographic and biostratigraphic analysis are marked in red circle.

EEI pseudo logs were extracted from the inversion volumes. The pseudo logs were then plotted together with the original well logs to see the match. Figure 11 shows a generally good match between the inversion pseudo logs and the well log data indicating good inversion results. The crossplot between the filtered well log and the inversion pseudo log shows a cross correlation of 85% for EEI and 97% for AI.

However, the sands encountered by the Abo Abo-A1X well are thin, where the thickest sands are only about 8m to 16m. These sands are below the seismic resolution ($\lambda/4$) which is about 32m ($\lambda = V/f$, where V = 3200m/s and f = 25Hz). Therefore, some of the thinner sands were not captured by the inversion results as these are significantly below the tuning thickness.

As the brine sands cannot be discriminated from the shales, it is also difficult, if not outright impossible, to determine sand body geometries and interpret potential depositional patterns. This is further complicated by the episodes of thrusting in the study area which displaced the lithologies away from their original depositional

configuration.

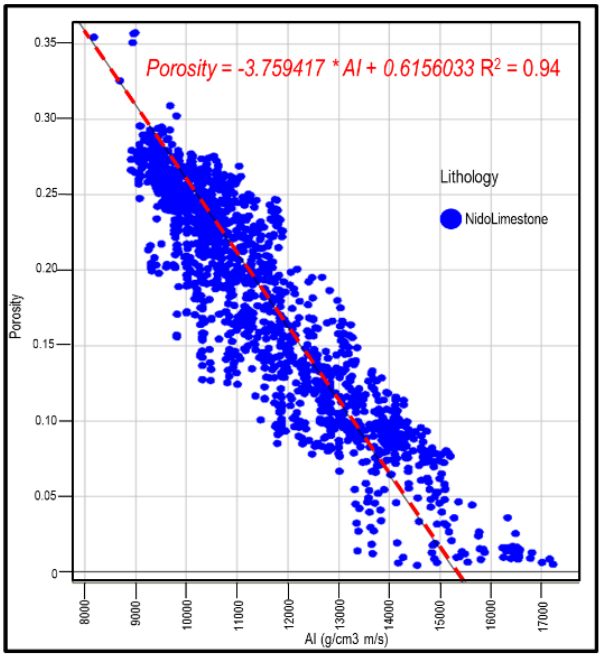

Figure 9. AI vs Porosity crossplot for the Nido Limestone

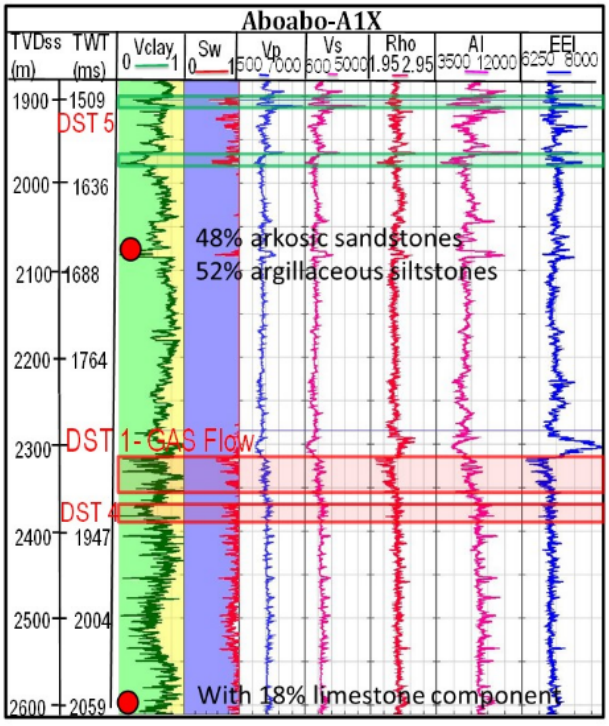

Figure 10. Seismic to well tie for Aboabo-A1X.

Figure 12 shows the AI horizon slice corresponding to the depth where gas flowed from the Abo Abo-A1X well while the EEI horizon slice is displayed on Figure 13. The low AI bodies are colored in green whereas high AI bodies are colored in blue and represents the limestones within the Pagasa Formation. For the EEI map, the low values are colored in red whereas the highs are in green. A section across the Abo Abo-A1X well is displayed in Figure 14. The AI and EEI volumes are co-rendered to highlight the low EEI gas sands (red), low AI and high EEI gas sand (green), limestones (blue), and brine sand and shale (brown). The map and the sections reveal the limited lateral extent of the gas sands encountered in the Abo Abo-A1X well. The inversion results also may have not captured the thin sands encountered by the well as they are significantly below the seismic resolution, as described above. Southeast of the Abo Abo-A1X well, some prominent low EEI bodies (red) can be seen and are highlighted by a red dashed oval (Figure 14). These bodies appear to be stratigraphically trapped as no apparent structural closure is observed in the section.

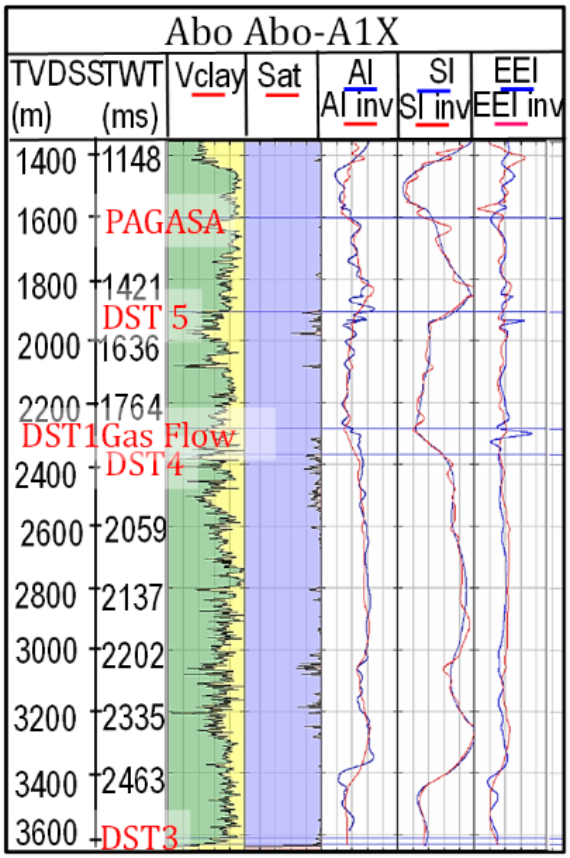

Figure 11. Comparison of the filtered well logs (blue) and the inverted pseudo logs (red).

An AI-EEI co-rendered section across the Baragatan-1A is displayed in Figure 15a. The limestones which were encountered in the well can be seen in the section as blue colored bodies. These limestone units appear as bright (high amplitude) anomalies on the seismic data (Figure 15b) and were predicted as gas charged sands in the Baragatan-1A well prognosis. An inversion study conducted prior to drilling of the well may have helped to correctly recognize these amplitude anomalies as limestone units instead of sands thereby de-risking the targets.

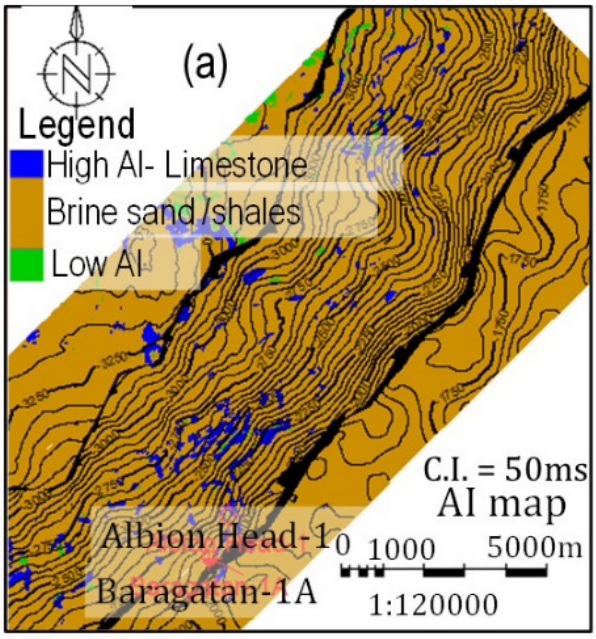

Figure 12. AI horizon slice corresponding to the sand that flowed in the Abo Abo-A1X well.

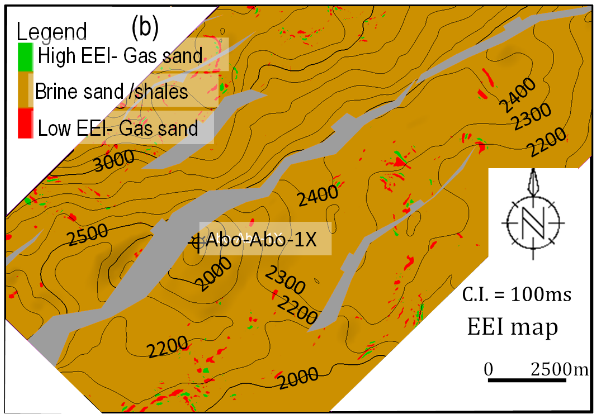

Figure 13. EEI horizon slice corresponding to the sand that flowed in the Abo Abo-A1X well.

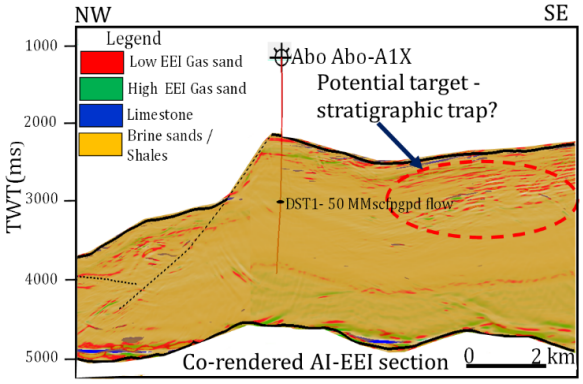

Figure 14. Co-rendered EEI-AI section across the Abo Abo-A1X well.

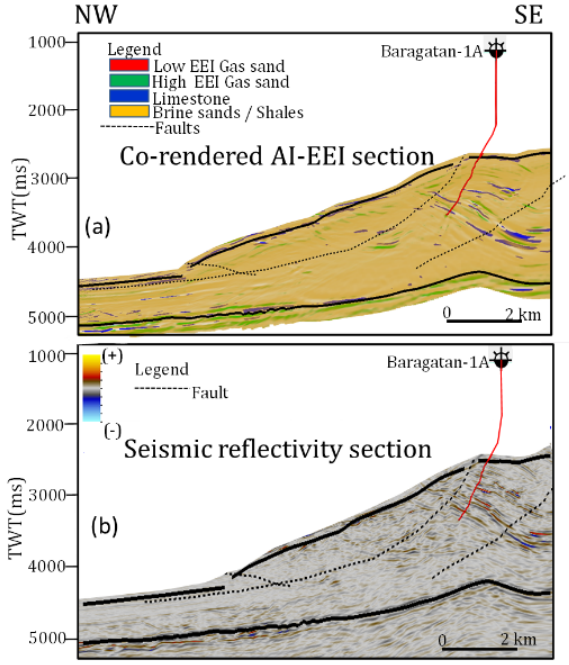

Figure 15. Co-rendered EEI-AI section across Baragatan-1A (a), seismic reflectivity section (b).

4.1.2 Seismic Inversion in the Nido Formation

The seismic-to-well tie of the Santiago-A1X well to the 2D seismic line SC6307-31 is shown in Figure 16. A very good well tie was achieved, with a correlation coefficient of 0.78. The inverted AI volume was converted to porosity using a linear transform marked as a red dashed line in Figure 9.

The two-way time (TWT) structure map of the top of the Nido Limestone is shown in Figure 17 while the P-impedance map is shown in Figure 18.

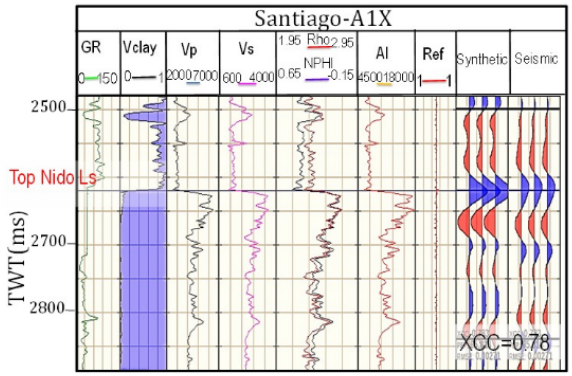

Figure 16. Seismic to well tie in Santiago-A1X well.

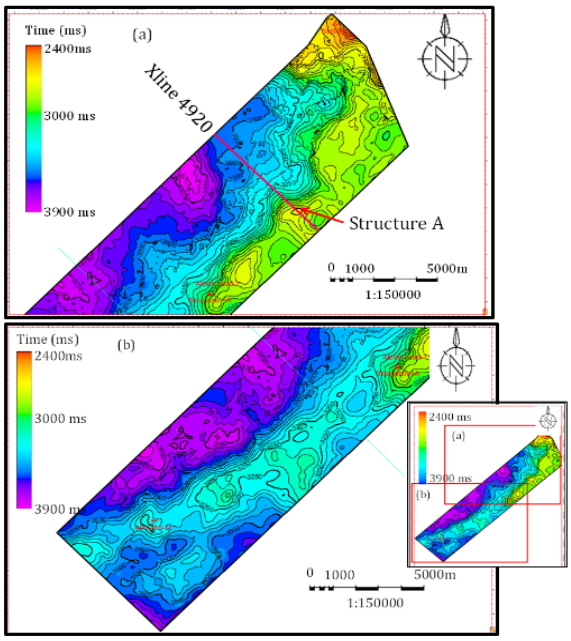

Figure 17. Top Nido Limestone Time Structure Map. C.I = 50ms

Several undrilled structural closures can be seen on the maps and these are oriented more or less in a SW-NE direction. The closure at the northeastern edge of the map was tested by the Santiago-A1X well. A closure located northeast of the Albion Head-1 well, marked as Structure A on the maps, is one of the closures that have been identified. An inverted AI section across Structure A is shown in Figure 19a, while Figure 19b shows the porosity prediction. The sections show that Structure A has porosities ranging from 5 to 25% at the crest of the structure. Similar range of porosities could also be seen at the flank of the structure. This range of porosities is consistent with seismic inversion results in NW Palawan (Borbajo, 2010). Structure A appears to have good reservoir properties and should be further evaluated as reservoir property prediction is just one of the elements in the petroleum system analysis.

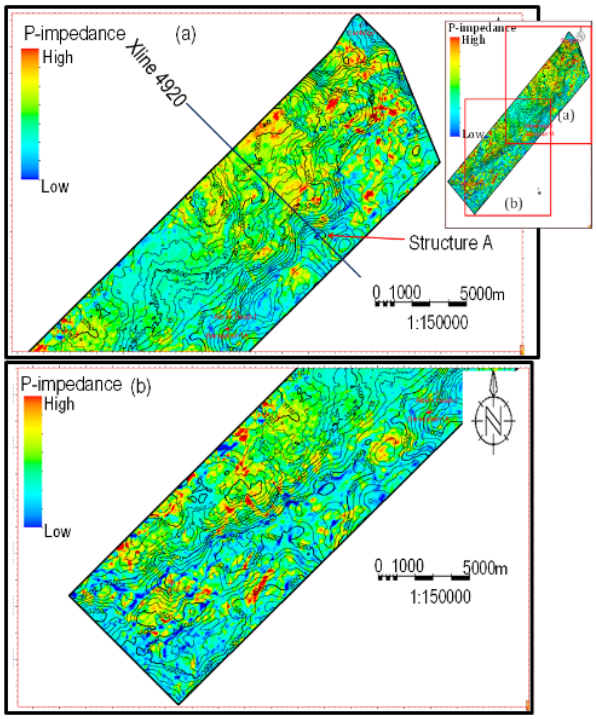

Figure 18. Top Nido Limestone AI Map. C.I. = 50ms

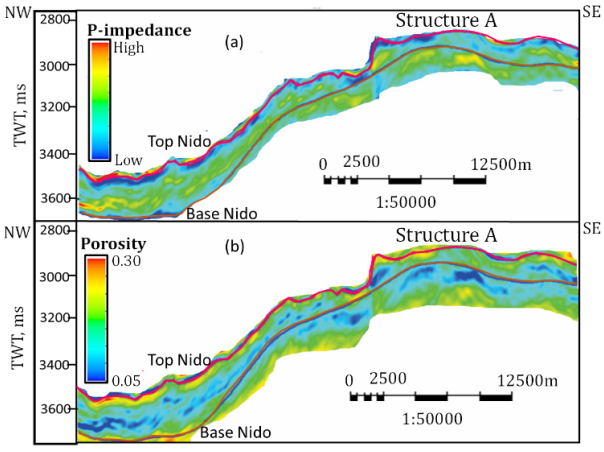

Figure 19. AI (a) and predicted porosity (b) sections across Structure A.

5. Conclusions

The rock physics analysis and seismic inversion conducted in the study area has revealed the following:

- The carbonate intervals within the Pagasa Formation can be distinguished by their very high AI. These appear as high amplitude reflectors in the seismic data.
- The gas-bearing sands, brine sands, and shales cannot be distinguished from each other in the normal incidence angle domain as their acoustic properties (AI, SI, and Vp/Vs) overlaps.
- Generating the EEI logs allows for better separation of the gas sands with brine sands and shales when AI is cross plotted with EEI at chi angle 25.
- Two types of gas sands were identified. The first type corresponds to low AI and high EEI, while the second type relates to moderate AI and low EEI and correlates to the interval that flowed 50 MMscfgpd of gas in the Abo Abo-A1X well.
- The higher AI in the second type of gas sand could be brought about by the presence of limestone fragments in the sands as seen from petrographic analysis in the Abo Abo-A1X well.
- Simultaneous seismic inversion and the generation of EEI are required to identify potential areas of gas sands within the seismic data. The sands in the Pagasa Formation that were encountered by the Abo Abo-A1X and Albion Head-1wells are generally thin and below the seismic resolution, while the gas sands identified in the simultaneous seismic inversion results have limited lateral extents.
- P-Impedance seismic inversion is an effective tool that can be used to identify areas with higher porosities in the Nido Limestone.
- Low AI values in the Nido Limestone can be correlated to higher porosities while higher AI values are associated with lower porosities. This predictable relationship between P-Impedance and carbonate porosities is similar to the reported character of the Nido Limestone in the Northwest Palawan Basin.

6. Acknowledgements

My heartfelt thanks to Dr. Joseph Lambiase and the Petroleum Geoscience program, for giving me a scholarship and the opportunity to pursue my graduate studies. I would also like to thank PNOC EC for supplying all the data used in my project. My deepest gratitude goes to Dr. Mirza Naseer Ahmad for his supervision and guidance, and to Monina and Jeff of PNOC EC for all their invaluable assistance and support. Finally, this work is dedicated to my very supportive husband, Renato, and my beloved son, Elessar Kyle.

7. References

Borbajo, R.M., 2010, Reservoir Characterization of the Nido Limestone in the Northwest Palawan Basin using Seismic Inversion: A research Report submitted as partial fulfillment for the Degree of Master of Science in Petroleum Geoscience at Chulalongkorn University, Thailand.

Connolly, P., 1999, Elastic impedance: The Leading Edge, 18, No.4, 438–452.

Fatti, J. L., Smith, G. C.,1994. Detection of gas in sandstone reservoir using AVO analysis: A 3-D seismic case history using Geostack technique: Geophysics, Vol.59, No.9; 1362-1376

Forbes, M.T., Mapaye, C.B., Bacud, J.A., 2011. Structural characterization of offshore Southwest Palawan, Philippines using the most recent 2D/3D seismic data. In Proceedings of the Southeast Asia Petroleum Exploration (SEAPEX) Meeting, Manila, Philippines, 6 April 2011.

Fournier, F., and J. Borgomano, 2007, Geological significance of seismic reflections and imaging of the reservoir architecture in the Malampaya gas field (Philippines): AAPG Bulletin, 91, 235–258.

Shuey, R.T., 1985, A simplification of the

Zoeppritz equations: Geophysics, 50, 609-614.

Smith, G.C., and Gidlow, P.M., 1987, Weighted stacking for rock property estimation and detection of gas: Geophys. Prosp.,35, 993-1014.

Steuer, S., Franke, D., Meresse, F., Savva, D., Pubellier, M., Auxietre, J.-L. and Aurelio, M., 2013. Time constraints on the evolution of the southern Palawan Island, Philippines from onshore and offshore correlation of Miocene limestones. Journal of Asian Earth Sciences.

Whitcombe, D.N., Connolly, P.A., Reagan, R.L. and Redshaw, T.L., 2000, Extended elastic impedance for fluid and lithology prediction: 70th Ann. Internat. Mtg., Soc.Expl. Geophys., Expanded Abstracts.

Whitcombe, D. N., 2002, Elastic impedance normalization: Geophysics, 67, 60-62.